

# Surface motion of a plane liquid jet

## *Ecoulement d'un jet liquide plan*

S.K.A. Naïb

B.Sc. (Eng.), Ph.D., A.C.G.I., D.I.C., C.Eng., F.I.C.E.  
Head of Department of Civil Engineering  
North East London Polytechnic

### Introduction

The jet from an overflow weir or from the orifice between the gates of a regulating sluice on entering the pool of water downstream, either flows along the surface, or alternatively is deflected downwards becoming fully submerged and sweeps along the bed of the pool, Figure 1. Both flows seem fairly stable; intermediate ones seldom occur. When the flow is reduced by increasing the downstream water level, submerged flow may suddenly change over to surface or wavy motion and vice versa.

A schematic section of the surface motion of the jet is shown in Figure 2. The jet flows over the slow moving fluid in the pool and is confined by a lower boundary. The flow consists of two parts: the potential core near the inlet enclosing a prism of fluid in which the velocity is uniform and equal to the initial value  $U_0$ , and the fully developed jet where the surface

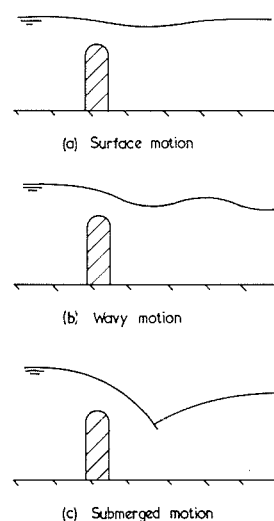


Figure 1 – Types of Flow Downstream of a Weir

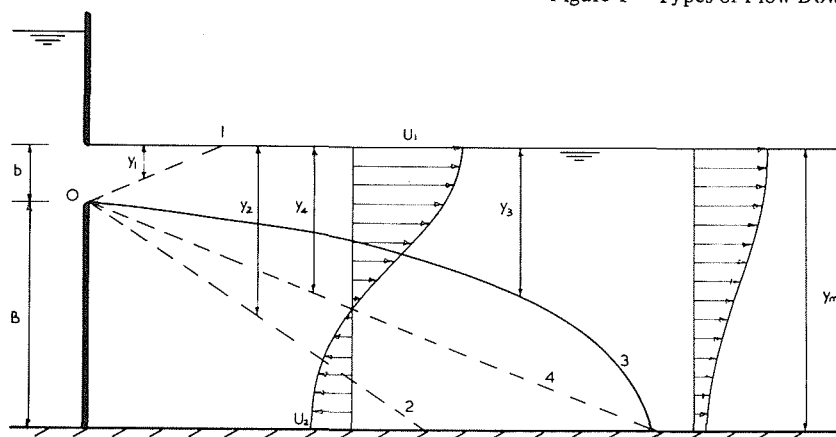


Figure 2 – Surface Motion of a Plane Liquid Jet

stream and the slow moving fluid in the pool below form a turbulent mixing region with an inner boundary O1 and an outer boundary O2. In the latter region, the velocity profile consists of a mixing layer with a maximum velocity  $U_1$  at the water surface and a counterflowing layer with a maximum reverse velocity  $U_2$  near the bed of the pool.

The mixing process between the surface stream and the surrounding fluid causes part of the latter to be carried forward with the jet under conditions in which both the forward momentum and the total discharge are conserved. The process of entrainment leads to recirculation to replace the fluid entrained and a zone of circulation motion is established underneath the surface stream. The line O3 defines the meanflow line bounding the fluid which is sucked outward from the stream.

The behaviour of such a jet is of importance in the design of partially submerged orifices, regulators, weirs, sedimentation tanks and fish passes of the pool type; yet very little information has been published on the flow. In their investigation of fish passes, Nemenyi and White [1] observed the flow over a weir and found that the surface profile had very little effect upon the change from surface to submerged motion, and that the principal factor was the thickness of the weir. The present research was undertaken partly to provide information for the design of stilling basins downstream of moveable canal regulators, and partly to lead to a better understanding of the complex behaviour of confined jets and streams under investigation by the author [2 to 8].

### Analytical approach

The physical aspects of dispersion of a surface jet has similarity with the mechanism of a plane submerged jet and the confined flow in the circulation zone behind the two-dimensional bluff body. A knowledge of the behaviour of such flows is therefore of importance in explaining the more complex motion of the surface jet. For the plane jet, Tollmien [9] found that in the region of potential core the inclination of the streamlines forming the limits of the jet are : (i) boundary on the uniform stream side expands at an angle of 1 in 12; (ii) boundary on the fluid at rest side expands at an angle of  $9.8^\circ$ . In the region of fully developed flow, half of the width of the mixing zone is given by:

$$b = 0.266 x \quad (1)$$

or with an angle of expansion of about  $15^\circ$  or 1 in 4. The central velocity at a distance  $x$  from the plane of the opening is given by

$$\frac{U}{U_0} = 3.64 \sqrt{\frac{b}{x}} \quad (2)$$

where  $U_0$  is the jet velocity at exit.

Abramovich [10] analysed the flow behind a two-dimensional bluff body and found the length of the circulation zone to be  $6.1 B$  where  $B$  is the half width

of the body and in the case of the surface jet it is the depth of the pool. This theory is correct as long as in the stream the core of constant velocity is retained throughout the length of the circulation zone, and as this core decays in a shorter distance, the theory becomes less accurate.

### Experimental conditions and methods

The experiments were conducted in a standard laboratory glass flume, 300 mm wide by 300 mm deep and 10 m long, having an outlet weir for adjusting the depth of flow, and a weighing arrangement for measuring the discharge. The flume was fitted with two perspex sheets, each 25 mm thick, to produce through a slit a surface water jet of depth  $b = 19$  mm and width 300 mm, as shown diagrammatically in Figure 2. The uniform velocity of the jet at exit was measured to be  $U_0 = 0.605$  m/s. The Froude number of the jet was calculated as

$$F = U_0/\sqrt{gb} = 0.605/\sqrt{9.81 \times 0.019} = 1.4.$$

The depth of the pool beneath the jet was  $B = 8 b = 152$  mm and it extended 8 m downstream of the jet exit. In comparison, the length of the recirculation flow in the pool was found to be about  $6 B = 912$  mm. All the results presented in this paper were deduced for this one jet, having the same density as the surrounding fluid.

The velocity distributions along the centreline of the flume were measured by a shielded dynamic probe [2]. The probe was found to be insensitive to direction changes through a range of angles of  $\pm 40$  degrees. The pressure distribution at any section of the flow was assumed hydrostatic and was locally measured by an accurate point gauge.

The velocities were also measured by a photographic technique developed by the author [11, 12]. For ease of photography, the experiments were carried out in a smaller glass flume, 100 mm wide by 300 mm deep and 3 m long, other dimensions of the flow remaining the same as above. The flume extended 2.75 m downstream of the jet exit. A mercury-vapour discharge lamp was used to produce a sheet of light 10 mm thick by 200 mm long along the centreline of the flume. By using a stroboscopic light, the paths of the illuminated oil tracers over successive periods of one-hundredth of a second were obtained as a series of dashed streaks, and by comparing the length between the centres of adjacent dashes with a linear scale included in the photograph, the magnitudes of velocities were obtained.

Typical photographs of the various regions of the jet are shown in Plates I, II and III. The local depth of flow is 171 mm and the flow is from right to left. The values of  $x/b$  approximately define the beginning and end of each photograph. A white scale is placed near the downstream end just above the water surface. The results obtained using such photographs were practically the same as those measured by the shielded probe. The reduction in width of flow from 300 mm to 100 mm apparently did not influence the distribution of velocities in the jet.

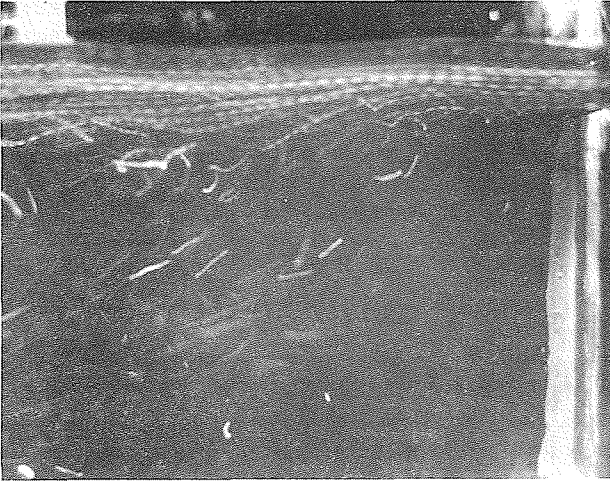


Plate I -- Flow Near Jet Exit,  $x/b = 0-12$ , Exposure 0.25 Second.



Plate II -- Flow in Entrainment Region of Jet,  $x/b = 12-24$ , Exposure 0.25 Second.

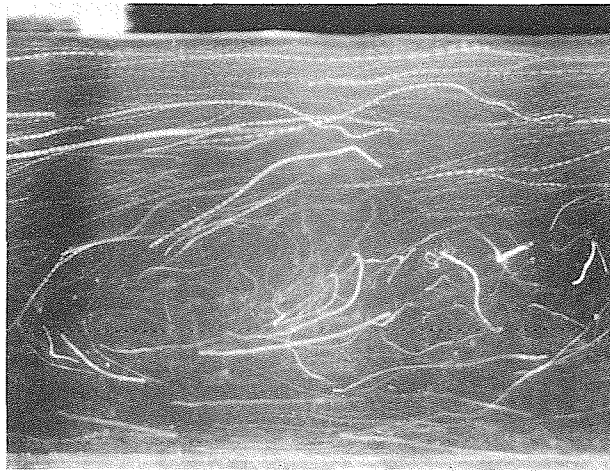


Plate III -- Flow in Recirculation Region of Jet,  $x/b = 30-42$ , Exposure 0.5 Second.

**Experimental results**

*Regions of Flow*

The results show that four regions are recognised along the direction of flow of the jet. These regions are mainly defined in the rate of decay of maximum stream velocity that exists just below the water surface, Figure 3. Region I of potential core extending to 8 widths from the outlet face, where the maximum velocity is constant and is equal to the original outlet velocity  $U_0$ . This distance is 4 widths shorter than that for the two dimensional free jet.

Region II of entrainment flow that extends to 28 widths, in which the maximum velocity varies inversely with distance from the outlet as given by:

$$\frac{U}{U_0} = 4.09 \sqrt{\frac{b}{x}} \quad (3)$$

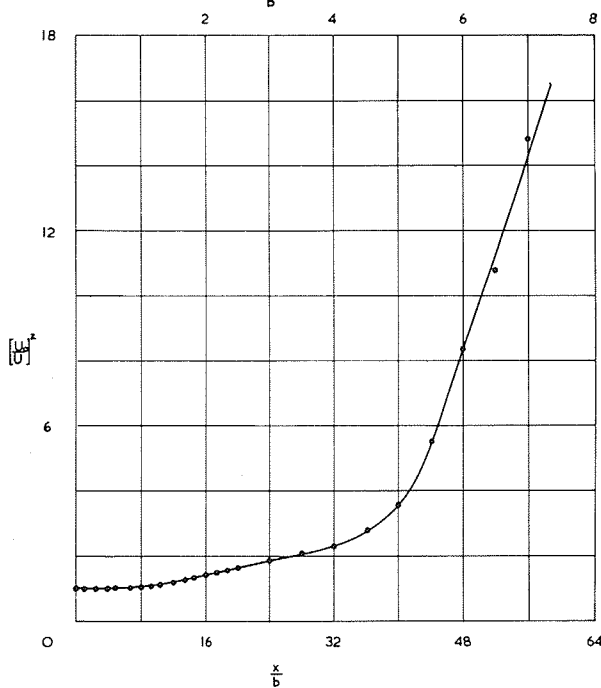


Figure 3 – Decay of Maximum Velocity

This is practically the same as that for the free plane jet except that the rate of decay is slightly faster. Region III of recirculated flow that extends to about 48 widths in which the flow is sucked from the jet into the circulation zone. The rate of decay of maximum velocity is variable due to the gradual rise in pressure in this region. Region IV of transformed flow which extends a long distance downstream and in which the expanded jet is transformed into a uniform rectangular stream for normal flow in an open channel. The rate of decrease of maximum velocity seems to vary inversely with  $x^{1/2}$ .

*Jet Boundaries*

Figures 4 and 5 show the water surface profile and boundaries of the jet plotted non-dimensionally. Apart from a slight reduction near the outlet, the depth remains constant up to about 28 widths, the point where the outer boundary O2 touches the bed of the pool. Further downstream the level gradually increases until it reaches the depth of flow in the channel. The slope of the water surface indicates the conversion of the kinetic head of the jet into potential head in Region III of recirculated flow.

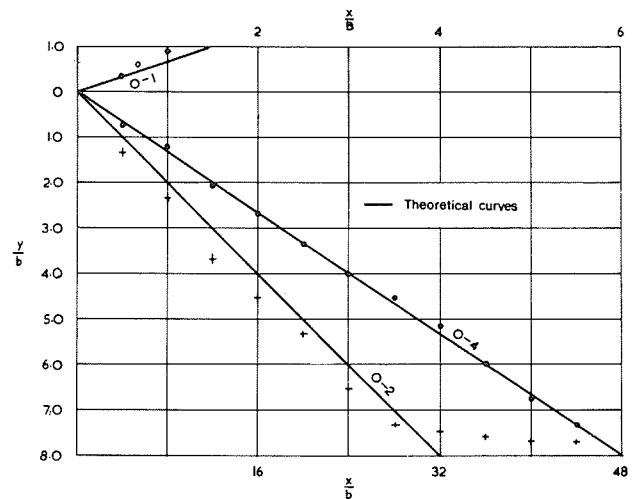


Figure 5 – Spreading of Jet Boundaries

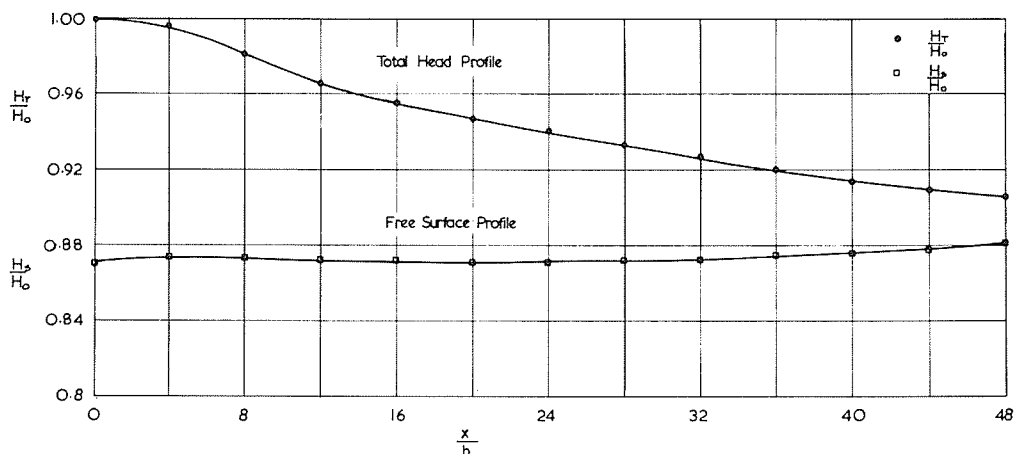


Figure 4 – Water Surface and Total Head Profiles

The inner boundary of the potential core is seen to expand at an angle of  $6.4^\circ$  or about 1 in 9, which is greater than that predicted for the boundary 01. The spreading angle of the outer boundary 02 is  $15.3^\circ$  and this is in agreement with Tollmien's value for the plane jet. The boundary 04 defined by  $u = 0$ , expands at an angle of  $9.4^\circ$ , again consistent with Tollmien's prediction. Where the boundary 03 reaches the bed a stagnation point is formed, marking the end of the circulation zone. The length of this zone is about six times the depth of the pool, compared with Abramovich's theoretical value of  $6.1 B$ .

**Velocity Distributions**

The velocity profiles in various regions of the jet are shown in Figures 6 and 7. In the region of entrainment the profiles are similar and are in satisfactory agreement with Tollmien's curve. Further downstream the profiles are still largely similar; the actual velocity falls faster on the stream side but slower on the circulation side than given by the theoretical curve. This is undoubtedly due to the pressure rise along the surface of the jet and to the curtailment of jet boundary 02 in this region. The variation of the maximum reverse velocity in the backflowing stream is given in Figure 8. The velocity reaches a peak value of  $0.4 U_0$  at  $x/L \cong 0.6$ , the end of the entrainment region of the circulation zone. Due to the relatively short potential core, the results are not in agreement with Abramovich's curve. However, they can be approximated by a sine curve as follows:

$$\frac{U_2}{U_1} = 0.30 \sin\left(\frac{\pi x}{L}\right) \quad (4)$$

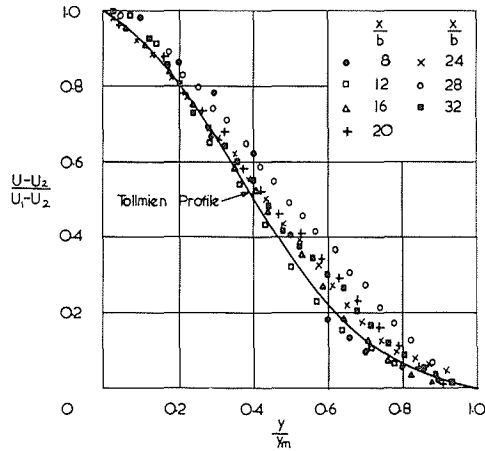


Figure 6 – Velocity Profiles in Region of Entrainment

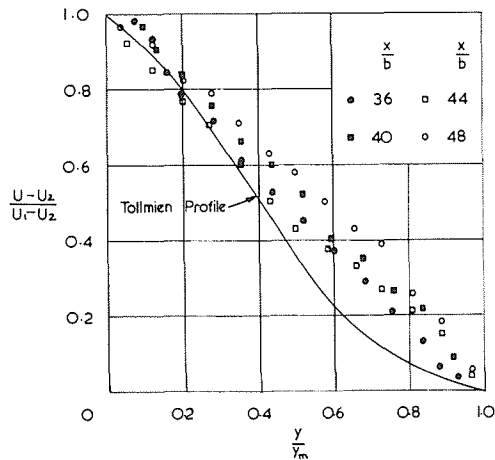


Figure 7 – Velocity Profiles in Region of Recirculation

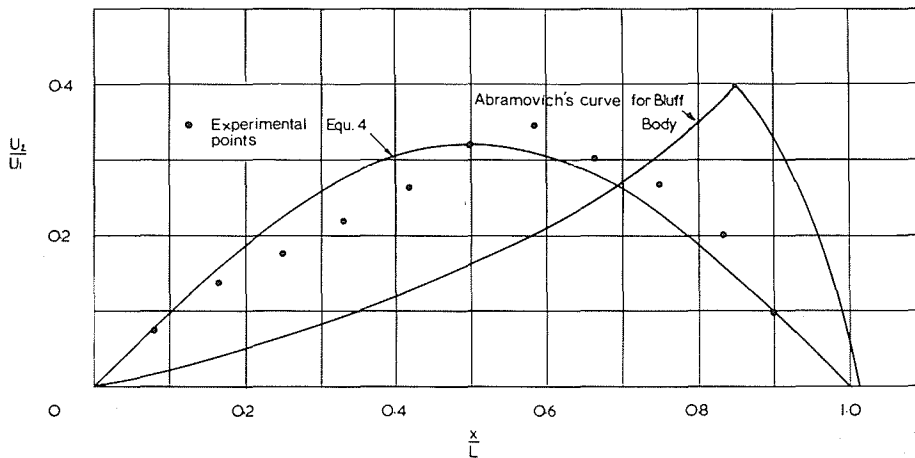


Figure 8 – Variation of Maximum Reverse Velocity

Further analysis led to the surprising results shown in Figure 9, where it is seen that experimental data closely lie to a Gaussian distribution curve represented by the following equation:

$$\left(\frac{U_2}{U_1}\right)^2 = \frac{K_1}{\sqrt{2\pi}} e^{-\frac{t^2}{2}} - K_2 \quad (5)$$

where  $K_1 = 0.227, K_2 = 0.008$  and

$$t = \sqrt{5} \left(\frac{1-2x}{L}\right)$$

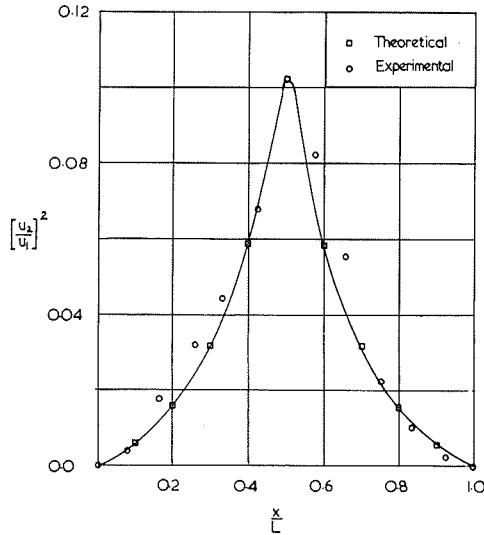


Figure 9 – Gaussian Distribution of Reverse Velocity

**Total Head Characteristics**

Due to the pressure rise in the region of recirculated flow it may be more appropriate to study the decay of the jet by considering the variation of total head along the direction of flow. At any vertical section of the mean flow, Figure 1, the total head is the sum of the static and kinetic heads and may be represented as follows:

$$H_T = H_s + H_k$$

or 
$$H_T = y + \frac{1}{2gq} \int_0^y u^3 dy \quad (6)$$

where  $y$  is the local depth of water and  $q$  is the unit discharge. Figure 10 shows the experimental results plotted as  $\log(H_T/H_0 + 1)$  against  $\log(x/b)$  where  $H_0$  is the total head of the jet at inlet. Downstream of the potential core, the straight line graph clearly indicates that for both the entrained and recirculated regions of the jet, the variation of total head is governed by the same power law, despite the pressure rise in the latter region, as given by the following expression:

$$\left(\frac{H_T}{H_0} + 1\right) = 2.10 \left(\frac{b}{x}\right)^{0.024} \quad (7)$$

It could therefore be said that for liquid jets diffusing under gravity the total head seems to be a more general parameter than the maximum velocity for studying the transformation of the jet within the whole of the circulation zone.

Another insight into the flow may be obtained by plotting the rates of static pressure head,  $dH_s/dx$ , of

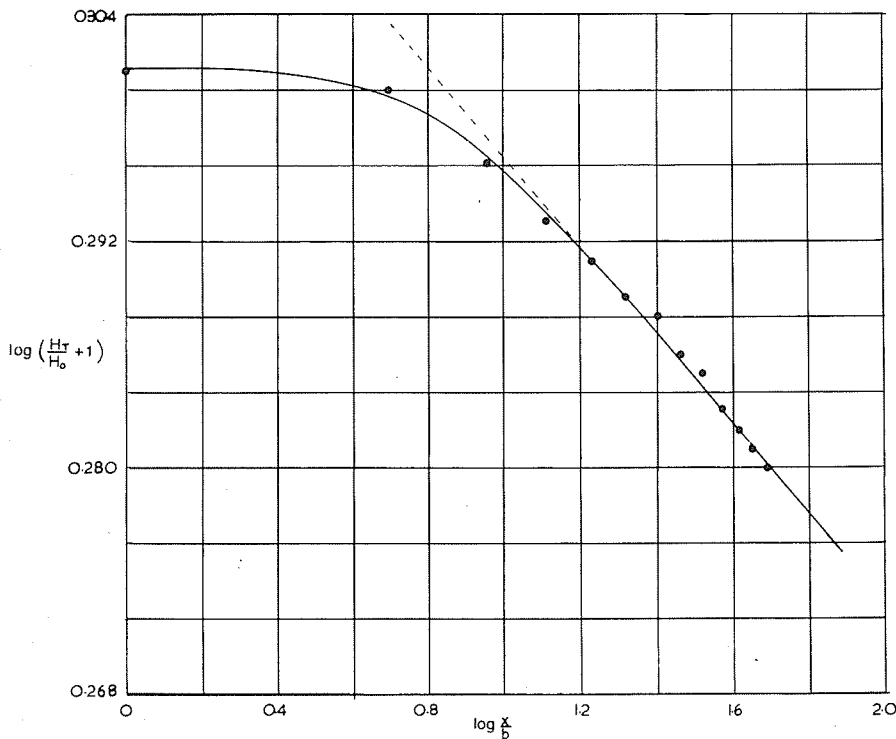


Figure 10 – Decay of Total Head

kinetic head,  $dH_k/dx$ , and of total head,  $dH_T/dx$ , with distance as shown in Figure 11. For the static head, the rate is small and constant in the entrainment region, then gradually decreases until the stagnation point is reached. The curves for the kinetic and total head rates are similar; both rates increase steeply to a maximum value just past the end of the potential core. Further downstream the rates decrease sharply, the two curves interesting near the end of the entrain-

ment region where the outer boundary of the jet (O2) reaches the bed of the pool. In the region of recirculation, the rate of dissipation of kinetic head remains surprisingly constant, while the rate for total head decreases gradually following a similar trend to that for the static head in the same region. This clearly indicates that the rate of dissipation is a maximum in the first half of the zone of diffusion.

## References

- [1] NEMENYI P. and WHITE C.M. – *Report on hydraulic research on fish passes : Appendix of Report of the Committee on Fish Passes*. Inst. Civil Eng., London, 1948.
- [2] NAIB S.K.A. – Mixing of a subcritical stream in a rectangular channel expansion. *J. Inst. Wat. E.*, Vol. 20, No. 3, p. 199, May 1966.
- [3] NAIB S.K.A. – Flow patterns in a submerged liquid jet diffusing under gravity. *Nature*, Vol. 210, p. 694, May 14, 1966.
- [4] NAIB S.K.A. – Unsteadiness of the circulation pattern in a confined liquid jet. *Nature*, Vol. 212, p. 753, Nov. 12, 1966.
- [5] NAIB S.K.A. – Abnormal grouping of large eddies in a submerged jet. *La Houille Blanche*, No. 3, p. 282, 1967.
- [6] NAIB S.K.A. – Stream boundaries of subcritical flow in a trapezoidal channel expansion. *Wat. & Wat. Eng.*, Vol. 73, p. 155, April 1969.
- [7] NAIB S.K.A. – Spreading and development of the parallel wall jet. *Aircraft Engineering*. Lond. p. 30, Dec. 1969.
- [8] NAIB S.K.A. – Deflexion of a submerged round jet to increase lateral spreading. *La Houille Blanche*, No. 4, p. 55, 1974.
- [9] TOLLMEN W. – *Calculation of turbulent expansion processes*. N.A.C.A., TM No. 1085, 1945.
- [10] ABRAMOVICH G.K. – *The theory of turbulent jets*. M.I.T. Press, Boston, USA, 1963.
- [11] NAIB S.K.A. – Photographic method for measuring velocity in a liquid jet. *The Engineer*, Lond., Vol. 221, p. 961, June 24, 1966.
- [12] NAIB S.K.A. – Measuring velocity in a liquid jet. *The Engineer*, Lond., Vol. 222, p. 236, Aug. 12, 1966.

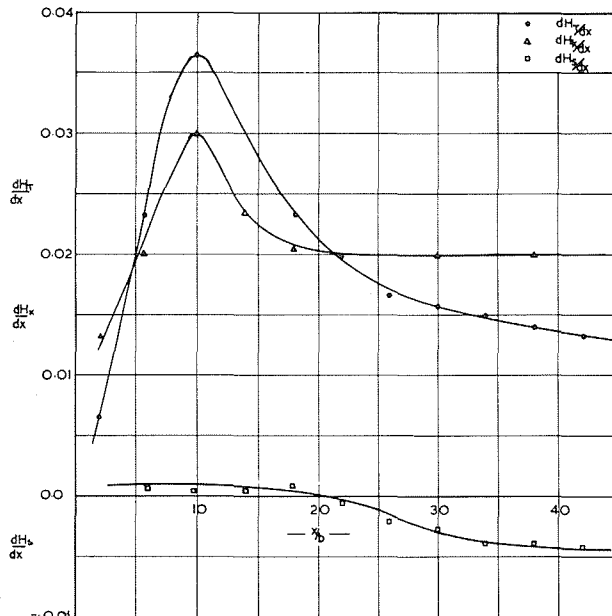


Figure 11 – Rates of Dissipation of Heads